

Metal-ions-coordinated Cross-linked Quasi-solid-state Polymer Electrolyte towards High Energy-density and Long-life Prussian Blue Analogs

Cathode

Xinyu Wang^{a,b}, Cheng Yang^{a}, Ning Jiang^{a,b}, Yichao Wang^{a,b}, Shouyu Sun^{a,b}, Yu Liu^{a*}*

^aShanghai Institute of Ceramics, Chinese Academy of Sciences

Shanghai 200050, China

^bUniversity of Chinese Academy of Sciences

Beijing 100049, China

*Email: yangcheng@mail.sic.ac.cn; yuliu@mail.sic.ac.cn

Supplementary materials

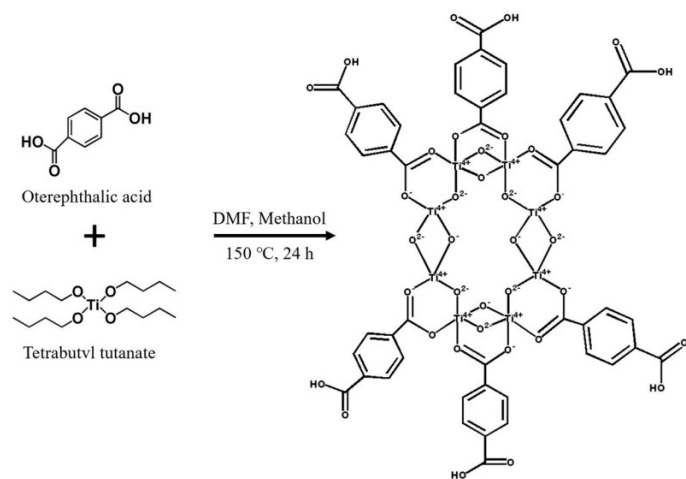


Figure S1 The synthetic route of MLI-125(Ti) by the solvothermal method¹.

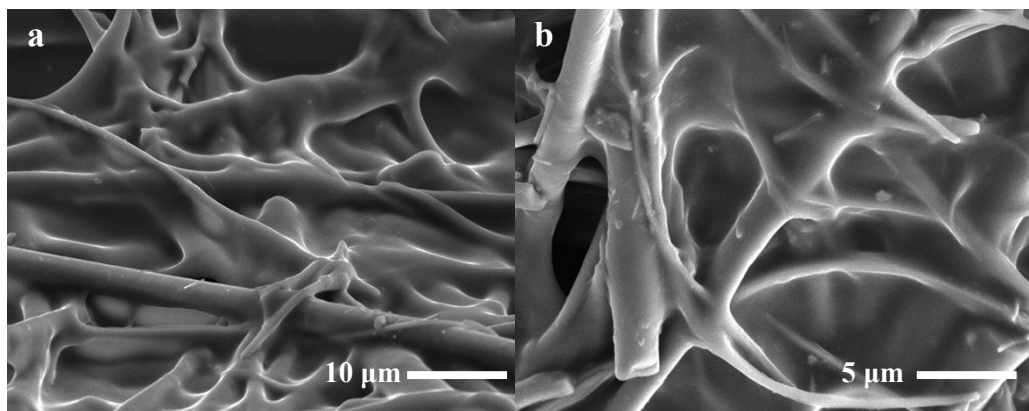


Figure S2 The SEM images of the cross-section of Ti@GPE.

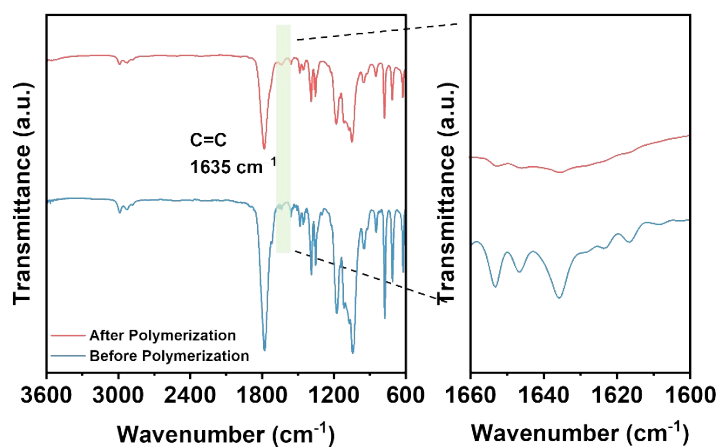


Figure S3 The FT-IR spectra of GPE polymer electrolyte before and after thermal polymerization.



Figure S4 The optical photographs of the precursor solution before (a) and after (b) thermal polymerization.

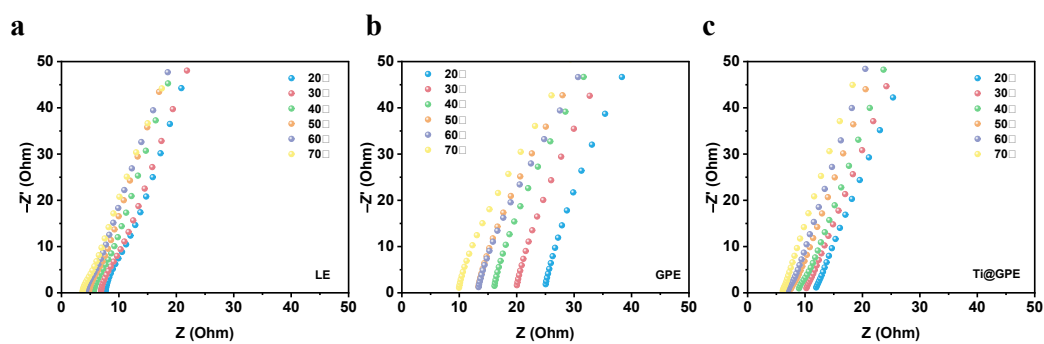


Figure S5 The ionic conductivity of different electrolytes at different temperatures (from 293 K to 343 K).

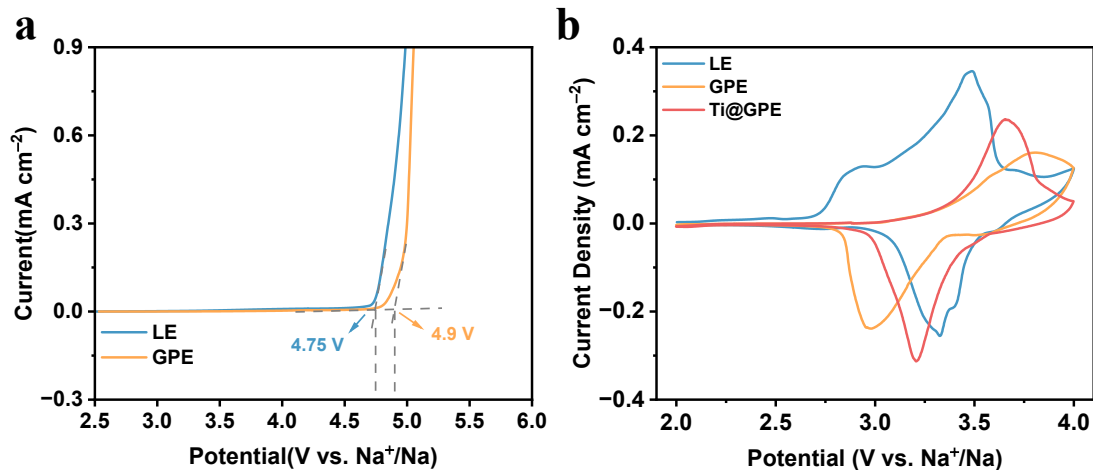


Figure S6 The LSV and CV tests at 0.2 mV/s of different electrolytes at room temperature.

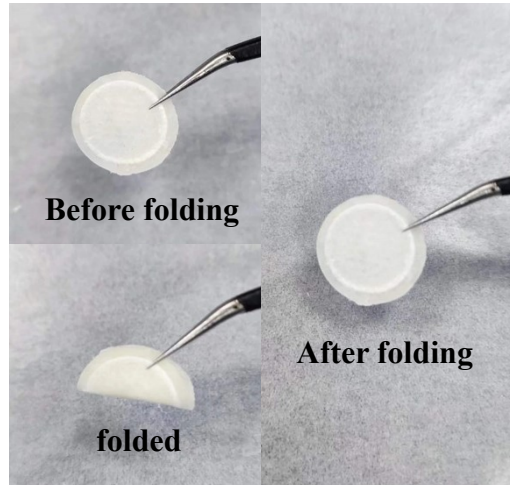


Figure S7 The optional photographs of the liquid precursor solution loaded on glass fibers (precursor solution@GF) after polymerization.

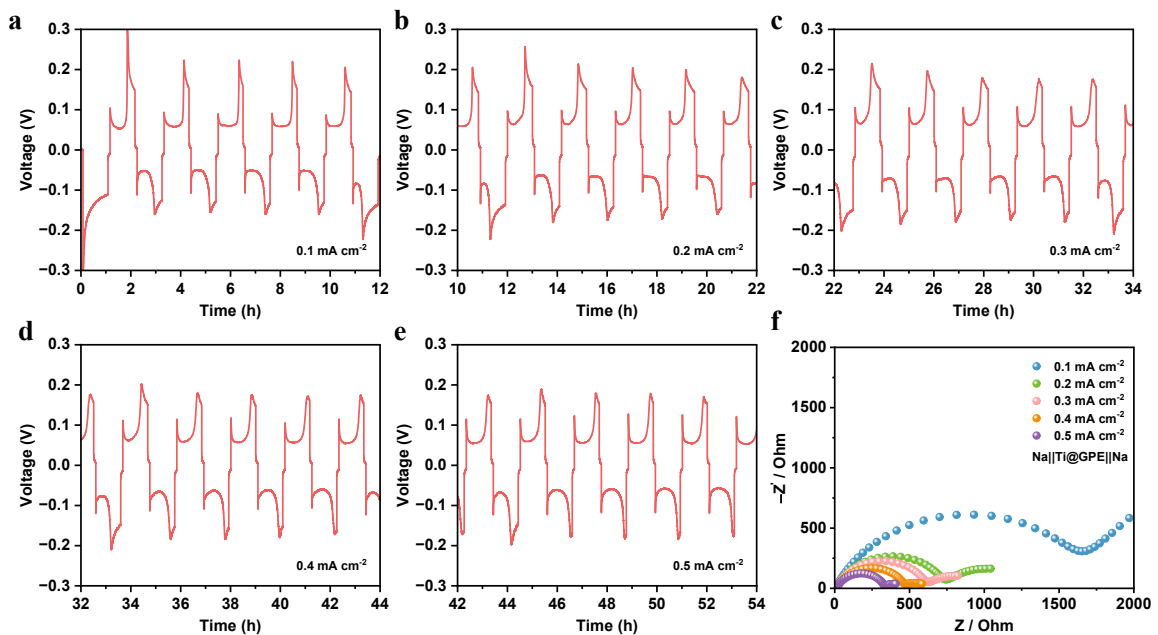


Figure S8 The peak magnification diagrams of $\text{Na}||\text{Ti}@\text{GPE}||\text{Na}$ symmetric cells under a) 0.1 、b) 0.2 、c) 0.3 、d) 0.4 、e) 0.5 mA cm^{-2} and d) the corresponding impedance of the symmetric battery under different current densities.

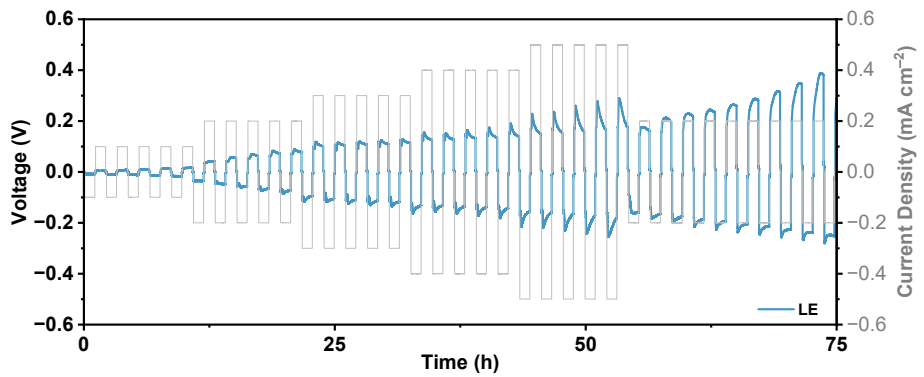


Figure S9 The variable current cycling tests of $\text{Na}||\text{LE}||\text{Na}$ symmetric battery.

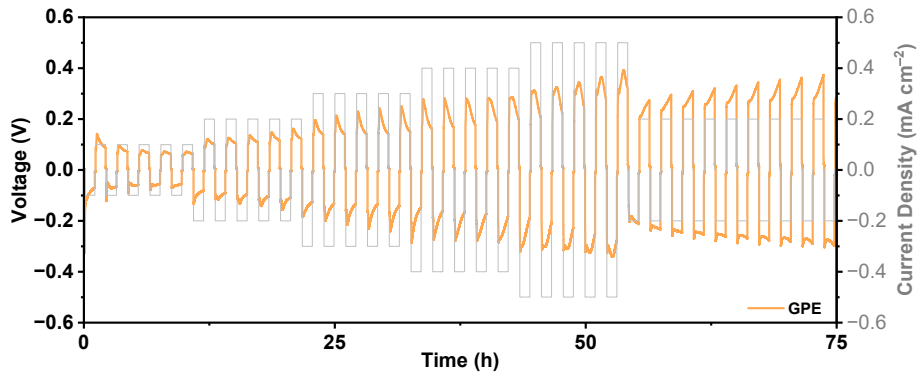


Figure S10 The variable current cycling tests of $\text{Na}||\text{GPE}||\text{Na}$ symmetric battery.

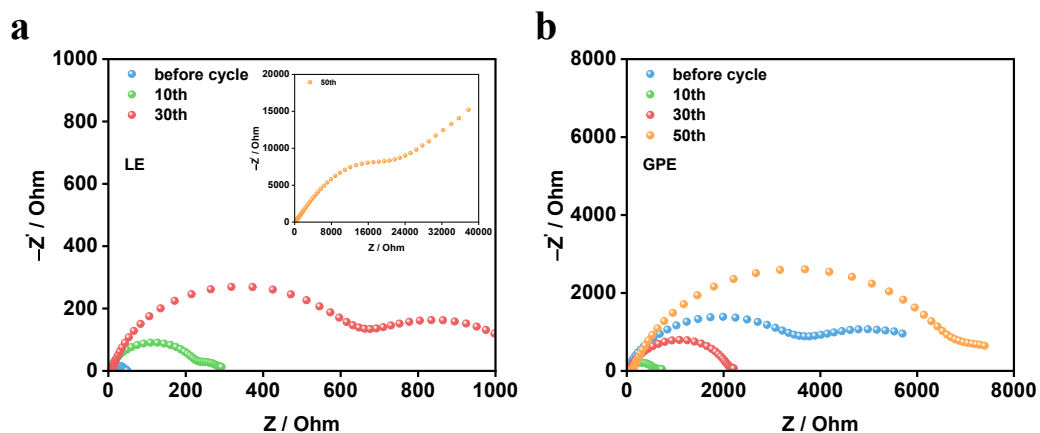


Figure S11 The electrochemical impedance spectroscopy (EIS) of $\text{Na}||\text{LE}||\text{Na}$ (a) and $\text{Na}||\text{GPE}||\text{Na}$ (b) symmetric batteries after various cycling times.

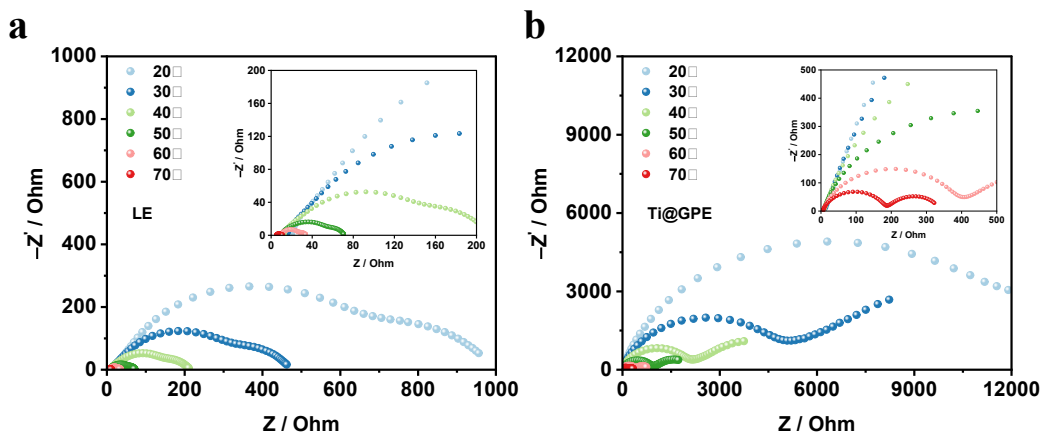


Figure S12 The EIS curves of $\text{Na} \parallel \text{LE} \parallel \text{Na}$ (a) and $\text{Na} \parallel \text{Ti}@\text{GPE} \parallel \text{Na}$ (b) at different temperatures (from 293 K to 343K).

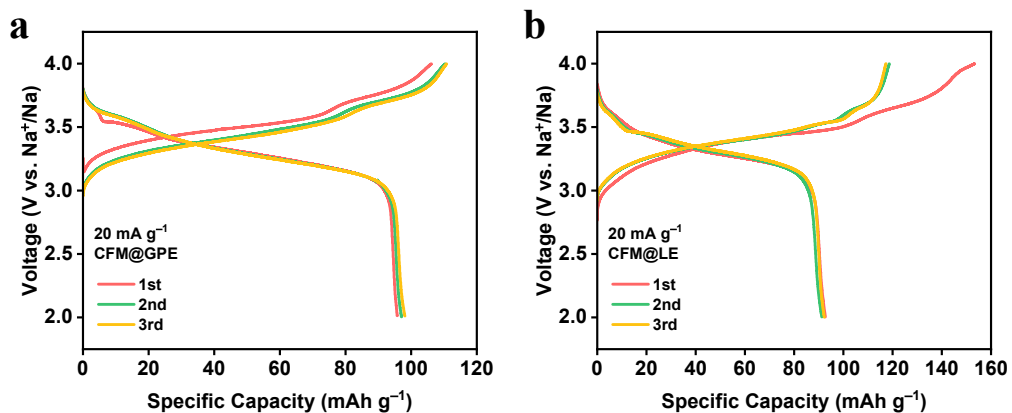


Figure S13 The initial three-cycle charge-discharge curves of CFM-PBAs||Na full batteries with GPE (a) and LE (b) electrolyte at 20 mA g^{-1} .

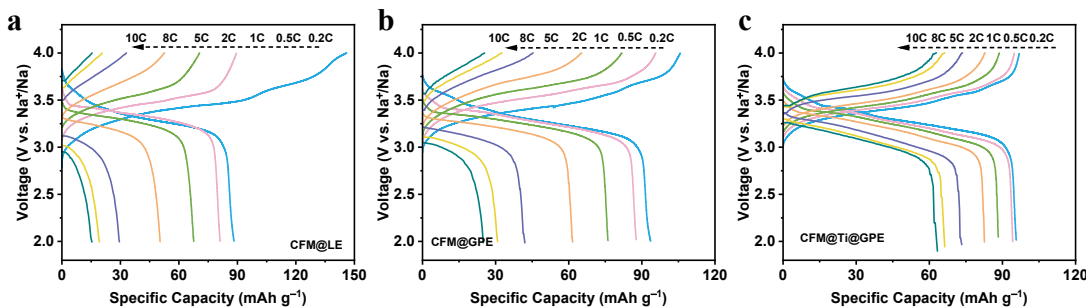


Figure S14 The charge-discharge curves of LE (a), GPE(b) and $\text{Ti}@\text{GPE}$ (c) electrolytes at different current density.

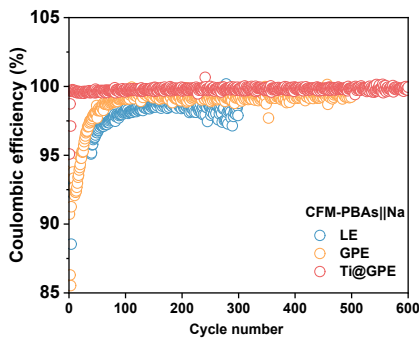


Figure S15 The coulombic efficiency of CFM-PBAs||Na batteries in different electrolytes with charging voltage of 4 V at 100 mA g⁻¹.

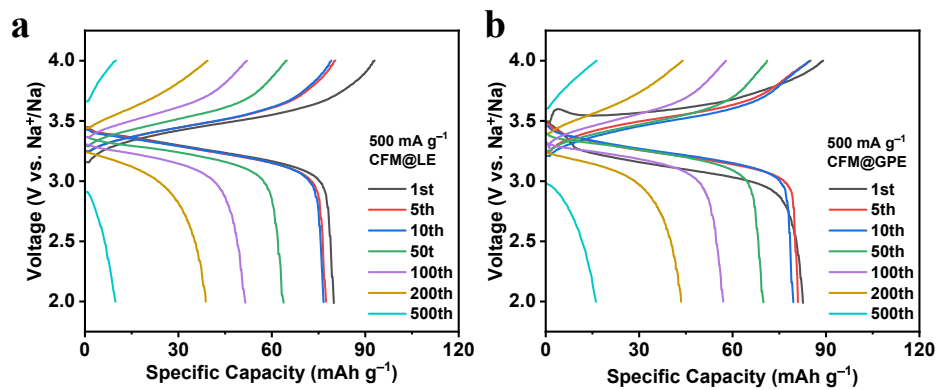


Figure S16 The charge-discharge curves of CFM-PBAs||Na full cells with different electrolyte systems at a current density of 5C, a for LE electrolyte and b for GPE electrolyte at 5C.

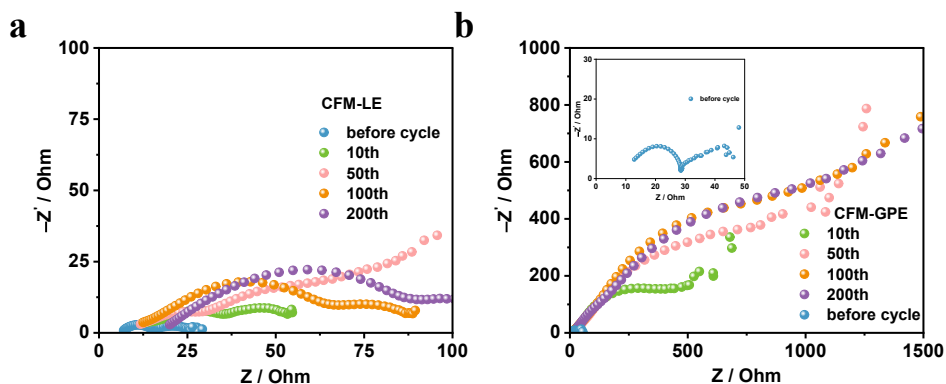


Figure S17 The electrochemical impedance spectroscopy of CFM-PBAs||Na full batteries in LE (a) and GPE (b) electrolytes.

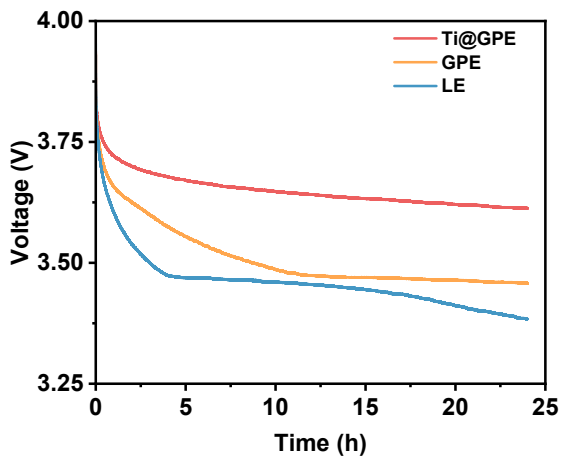


Figure S18 The static discharging curves of CFM-PBAs||Na charged to 4.0 V for 24 h.

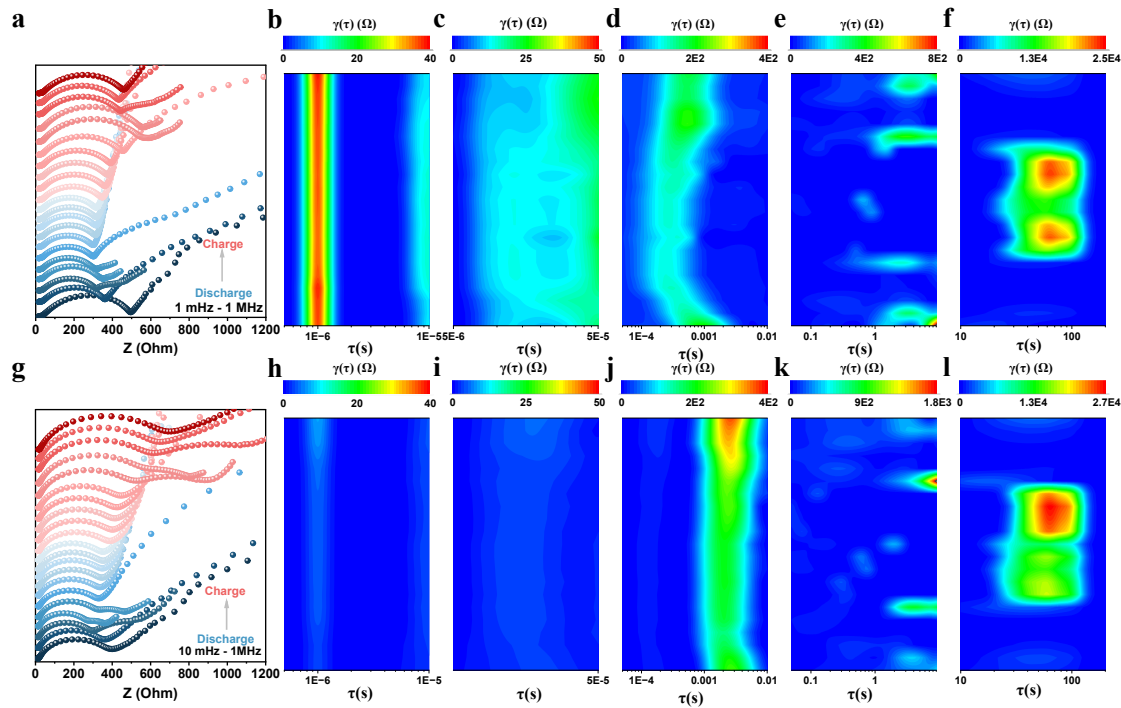


Figure S19 In-situ EIS during the first cycle of a) GPE and g) LE electrolyte. The total timescale distributions of different kinetics processes of b-f) GPE and h-l) LE electrolyte.

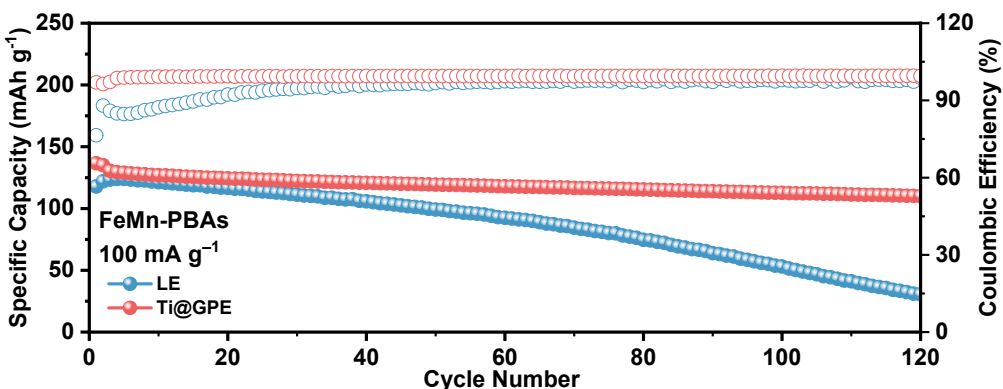


Figure S20 The cycling performance of FM-PBAs||Na full batteries in LE (a) and Ti@GPE (b) electrolytes at current density of 100 mA g^{-1} .

Table S1 The ionic conductivity and tensile performance comparison of different quasi-solid-state polymer electrolyte

Electrolyte	Ionic conductivity $\times 10^{-4} \text{ S cm}^{-1}$	Tensile strength MPa	Source
ANI-82	4.3	10.1	2
v-NBR/TAC/IL	2.2	0.52	3
GDT@GF	1.19	8.7	4
PISSE60%	3.03	0.811	5
F-Mo ₂ C-LCPP	5.57	16.375	6
CNF/PEG	6.1	9.5	7
Ti@GPE	38.5	13.85	This work

Table S2 Relevant parameters for porosity in quasi-solid polymer electrolytes.

QSPE	Ti@GPE	GPE
Thickness (mm)	0.562	0.610
Mass before QSPE treatment (g)	0.7118	0.07225
Mass after QSPE treatment (g)	0.02347	0.02013
Content of plasticizer (%)	67	64
Porosity (%)	17.9	21.4

Table S3 Comparison of electrochemical performances of the as-designed Ti@GPE with other reported quasi-solid-state polymer electrolytes in Na||Na symmetric batteries.

Quasi-solid-state polymer electrolyte	Current density (mA cm ⁻²)	Capacity (mAh cm ⁻²)	Duration (h)	Reference
PLM@LE	0.6	/	300	8
ATFPE	0.1	0.1	600	9
PEGMEM-co-SSS@ZIF-8	0.5	/	230	10
PDA@PU-GPE	1	0.5	450	11
30%NZSP-PAN	0.1	/	400	12
PFSA-Na	0.5	/	300	13
PSB ₆₀ -GPE	0.5	/	800	14
ANI-82	0.4	/	350	2
Ti@GPE	0.1	0.1	800	This work

Table S4 Comparison of ionic conductivity and electrochemical performances of the as-designed Ti@GPE with other reported quasi-solid-state polymer electrolytes (use PBAs as the cathode).

Quasi-solid-state polymer electrolyte	Ionic conductivity (S cm ⁻¹)	Discahrge capacity at 0.2 C (mAh g ⁻¹)	Cycle rate	Cycles	Capacity and retention	Reference
30%NZSP-PAN	1.79*10 ⁻⁵	112	0.1C	200	90 93.71%	12
PEO20-KTFSI1	1.30*10 ⁻⁶	108	1/15 C	50	97 90%	15
PVDF-HFP/IL/PDA	1.09*10 ⁻³	113.4	0.2 C	100	99.4 87.7	16

PFSA-Na	1.78×10^{-4}	~130	1 C	1100	95 84.6%	13
ZHPE-50	8×10^{-2}	65	10 C	1000	15 75%	17
Ti@GPE	3.85×10^{-3}	92	5C	2000	72 78%	This work

References

- Q. Liu, L. Yang, Z. Mei, Q. An, K. Zeng, W. Huang, S. Wang, Y. Sun and H. Guo, *Energy Environ. Sci.*, 2024, **17**, 780-790.
- X. Dong, Y. Zhang, Z. You, Y. Chen, X. Wu and Z. Wen, *Adv. Funct. Mater.*, 2024, **n/a**, 2405931.
- D. Zhang, Y. Shi, J. An, S. Yang and B. Li, *J. Mater. Chem. A*, 2022, **10**, 23095-23102.
- Y. Sun, M. Pan, Y. Wang, A. Hu, Q. Zhou, D. Zhang, S. Zhang, Y. Zhao, Y. Wang, S. Chen, M. Zhou, Y. Chen, J. Yang, J. Wang and Y. NuLi, *Angew. Chem. Int. Ed.*, 2024, **n/a**, e202406585.
- J. Yang, R. Li, P. Zhang, J. Zhang, J. Meng, L. Li, Z. Li and X. Pu, *Energy Storage Mater.*, 2024, **64**, 103088.
- Y. Shan, L. Li, X. Chen, S. Fan, H. Yang and Y. Jiang, *ACS Energy Lett.*, 2022, **7**, 2289-2296.
- Z. Wang, P. Heasman, J. Rostami, T. Benselfelt, M. Linares, H. Li, A. Iakunkov, F. Sellman, R. Östmans, M. M. Hamedi, I. Zozoulenko and L. Wågberg, *Adv. Funct. Mater.*, 2023, **33**, 2212806.
- G. Zhang, J. Shu, L. Xu, X. Cai, W. Zou, L. Du, S. Hu and L. Mai, *Nano-Micro Letters*, 2021, **13**, 105.
- J. Guo, F. Feng, S. Zhao, R. Wang, M. Yang, Z. Shi, Y. Ren, Z. Ma, S. Chen and T. Liu, *Small*, 2023, **19**, 2206740.
- J. Zhang, Y. Wang, Q. Xia, X. Li, B. Liu, T. Hu, M. Tebyetekerwa, S. Hu, R. Knibbe and S. Chou, *Angew. Chem. Int. Ed.*, 2024, **63**, e202318822.
- Y. Zhang, H. Yuan, L. Shi, H. Lai, X. Wu and Z. Wen, *ACS Sustainable Chemistry & Engineering*, 2024, **12**, 3142-3152.
- T. Wang, M. Zhang, K. Zhou, H. Wang, A. Shao, L. Hou, Z. Wang, X. Tang, M. Bai, S. Li and Y. Ma, *Adv. Funct. Mater.*, 2023, **33**, 2215117.

13. G. Du, M. Tao, J. Li, T. Yang, W. Gao, J. Deng, Y. Qi, S.-J. Bao and M. Xu, *Adv. Energy Mater.*, 2020, **10**, 1903351.
14. H. Lai, Y. Lu, W. Zha, Y. Hu, Y. Zhang, X. Wu and Z. Wen, *Energy Storage Mater.*, 2023, **54**, 478-487.
15. A. D. Khudyshkina, P. A. Morozova, A. J. Butzelaar, M. Hoffmann, M. Wilhelm, P. Theato, S. S. Fedotov and F. Jeschull, *ACS Applied Polymer Materials*, 2022, **4**, 2734-2746.
16. M. Xie, S. Li, Y. Huang, Z. Wang, Y. Jiang, M. Wang, F. Wu and R. Chen, *ChemElectroChem*, 2019, **6**, 2423-2429.
17. S. Dilwale, P. P. Puthiyaveetil, A. Babu and S. Kurungot, *Small*, 2024, **n/a**, 2311923.